

MELTING BEHAVIOUR OF FELDSPAR PORCELAIN GLAZES

Roxana Lucia DUMITRACHE, I. TEOREANU*

Proiectarea compoziției glazurilor nefritate, pe baza fuzibilității acestora, în condițiile tratamentului termic rapid aplicat la fabricarea industrială a porțelanului feldspatic tare, trebuie să ia în calcul datele oferite de microscopia de temperatură ridicată, selectând compozițiile a căror perioadă inițială a topirii este deplasată la peste $\sim 1250^{\circ}\text{C}$, iar temperatura sfârșitului topirii se află în intervalul $1360\text{-}1390^{\circ}\text{C}$. Combinarea rezultatelor oferite de analiza termo-dilatometrică a glazurii și microscopia de temperatură ridicată, conduce la selectarea compozițiilor a căror viscozitate scade rapid, până la 1300°C , asigurându-se, astfel, obținerea unei suprafețe finale netede a glazurii.

The design of feldspar porcelain glazes compositions based on their fusibility, under fast firing conditions applied to industrial manufacturing of feldspar porcelain, must take into account the data provided by hot-stage microscopy (point of minimum base contact area with the substrate) above $\sim 1250^{\circ}\text{C}$ and the final stage of melting (the end of melting) in the range $1360\text{-}1390^{\circ}\text{C}$. Combining the results provided by thermal dilatometry analysis and hot-stage microscopy on glazes one can select the compositions whose viscosity decreases rapidly up to 1300°C and so obtaining a smooth final surface of glaze.

Keywords: glaze, feldspar porcelain, hot stage microscopy, melting, viscosity, surface tension

Introduction

The melting behaviour of feldspar porcelain glazes depends on the characteristics and homogeneity of the raw materials batch, with implications in kinetics of chemical reactions and achievement of thermodynamic equilibrium of oxide systems. During the heat treatment the glaze must be considered as a heterogeneous system changing its aggregation state and that is accompanied by structural changes of the formed melt and of its phase composition, as well [1].

The heat treatment (firing) temperature cannot be accurately determined using additive rule due to the complexity of the reaction process. However,

* Chemical engineer, SC ARPO SA, Curtea de Argeș, Prof., Dept. of Science & Eng. of Oxide Materials and Nanomaterials, Faculty of Applied Chemistry and Materials Science, University POLITEHNICA of Bucharest

Lengersdorff [2] has developed a procedure to calculate an approximate firing temperature in dependence of the so-called “flux factor”. This can be calculated using the relation:

$$F = \frac{\sum S_i f_i}{\sum S_j f_j} \cdot 100 \quad (1)$$

where: F is the flux factor; S_1, \dots, S_i are the molar fractions of the oxides having the Lengersdorff flux factor higher than 0.4 ($f_i > 0.4$), and S_1, \dots, S_j are the molar fractions of the oxides with $f_j < 0.4$.

Accordingly, the firing temperature is calculated as:

$$FT = (161.21789 - F) / 0.10252 \quad (2)$$

where: F is the flux factor calculated from equation (1), FT – the firing temperature (°C), and the constants within equation (2) were determined statistically by Lengersdorff.

Experimentally, one needs to determine with accuracy the end of melting temperature of the glaze. This can be higher with 50-100°C than the calculated one, due to the different way of defining the two temperatures.

The end point of melting temperature of a raw material mixture is given by the temperature at which a cylinder or cube become spherical under the action of the surface tension of the melt [3]. The end point of melting temperature of a glaze is always higher so that viscosity and surface tension of the melt allow it to extend on the substrate surface [4].

To form a flat, smooth layer, with no waves, the glaze must have an adequate fusibility in the conditions of the applied heat treatment. The ability of the glazes to form flat, smooth layers without flowing on tilted surfaces or divesting the edges depends on their viscosity and surface tension in molten state. However, surface tension cannot be considered independent of viscosity at any particular temperature. The resultant of simultaneous influence of viscosity and surface tension is determinant for the glaze ability to cover and hide surface defects, as well as for providing quality to gloss and texture of the final (fired) glaze surface. The flowing, i.e. the ratio between surface tension and viscosity represents a double function depending on firing cycle and chemical composition of glaze [5].

Viscosity is one of the glaze physical properties that show very well the structural changes of the melt. A silicate melt at its end point of melting temperature contains a large variety of anion units, among which exists a distribution of bonding-oxygen atoms. Important steps during the dissolution

process within a silicate melt are: diffusion of cations with high mobility, e.g. Na^+ , into an interstitial site of silica network; breaking of Si-O bondings in network around the integrated ion; joining of Si atoms unsatisfied bondings with nonbonding oxygen atoms into a structural unit of melt. The end point of melting temperature is therefore under the liquidus temperature with approximately 300°C , due to the “history of melting” [6].

Vogel-Fulcher-Tamman (VFT) equation [7] provides the variation of glaze viscosity with temperature (3), in good agreement with experimental data obtained for a large temperature range and, therefore is used for calculation of viscosity versus temperature for industrial glasses and glazes:

$$\log \eta = A + B/(T - T_0), \quad (3)$$

where η is the viscosity of melted glaze and A, B, T_0 are constants (their calculation and corresponding values are given in Appendix).

Surface tension of glazes depends on chemical composition and temperature. For tableware porcelain the surface tension of corresponding glazes, at maximum temperature of the heat treatment has values ranging between 300 – 400 mN/m. The behaviour of the melted glaze at the interface with the ceramic substrate, during the heat treatment is influenced by the surface tension and wetting angle. As concern the surface tension there were made rather comparative studies than direct search.

The composition of glaze, determining the value of surface tension, influences its wetting ability. Also, the wetting ability depends on the composition of the ceramic substrate. The wetting ability of the initial melt upon the surface grains of refractory oxides that exists in certain amounts in glaze composition influences the rate of glaze melting. The wetting ability of the melted glaze also influences the adhesions to the ceramic body, as well as the thickness of the intermediate layer ceramic substrate – glaze and smoothness of the fired glaze layer.

Dissolving takes more time and requires higher heat treatment temperatures when surface tension of melt is higher, so a less wetting of quartz grains from the batch. Reducing of surface tension may have important effects on melting rate of glaze raw batch, on reactions between components and elimination of non-homogeneous parts of glaze melt [8].

A lower surface tension favours the release and removal of gas bubbles during the heat treatment of glaze; a higher surface tension will favour the resorption of bubbles during the cooling of glaze. At the same time, lower surface tension favours the covering of ceramic surface with glaze and formation of smooth surface whilst higher surface tension can result in a rough surface and possible run of the glaze.

The firing curve, heating rate, temperature plateau, cooling and maximal firing temperature, as well and particularly the firing atmosphere influence

decisively the formation of ceramic substrate and glaze through heat treatment. The firing atmosphere has an important influence upon mechanism of bubble formation and the shade of the final product. A longer period of time of maintaining at maximum temperature, when keeping constant the conditions within the region of reducing atmosphere yields a product of higher quality [9, 10].

The glaze compositions design based on their fusibility, when fast firing conditions are applied (10°C/min, 5 hours cycle from cold to cold), at a maximum temperature of 1360-1390°C, in industrial kiln for hard feldspar porcelain, must consider the data provided by hot stage microscopy when selecting the compositions whose initial melting temperature (point of minimum base contact area with substrate) is shifted above 1250°C and the temperature for corresponding end point melting ranges between 1360-1390°C [11].

Combining the results provided by thermal dilatometry analysis and hot stage microscopy on glazes one can select the compositions whose viscosity decreases rapidly up to 1300°C and so obtaining a final smooth surface glazes.

1. Conditions and experimental procedures

There were studied eight industrial glazes for tableware hard feldspar porcelain, noted from A to H, mainly differing by SiO₂:Al₂O₃ ratio. The molar equivalents calculated according to Seger and compositional characteristics are listed in Table 1.

Table 1.

Compositional characteristics of glazes A-H

| | Glazes | | | | | | | |
|--|--------|-------|-------|-------|-------|-------|-------|-------|
| | (A) | (B) | (C) | (D) | (E) | (F) | (G) | (H) |
| SiO ₂ :Al ₂ O ₃ | 12.15 | 11.8 | 10.88 | 10.81 | 10.44 | 10.39 | 10.29 | 8.98 |
| Al ₂ O ₃ | 0.38 | 0.41 | 0.45 | 0.48 | 0.51 | 0.5 | 0.48 | 0.50 |
| Σ RO ₂ | 4.65 | 4.86 | 4.95 | 5.18 | 5.3 | 5.19 | 4.94 | 4.52 |
| Σ R ₂ O ₃ | 0.38 | 0.41 | 0.45 | 0.48 | 0.51 | 0.5 | 0.48 | 0.5 |
| Σ R ₂ O | 0.28 | 0.29 | 0.28 | 0.29 | 0.29 | 0.3 | 0.28 | 0.22 |
| Σ RO | 0.72 | 0.71 | 0.71 | 0.71 | 0.71 | 0.7 | 0.73 | 0.78 |
| Basic oxides [%] | 16.58 | 15.95 | 15.63 | 15.02 | 15.43 | 15.70 | 15.58 | 16.61 |
| Amphoter oxides [%] | 6.30 | 6.54 | 7.03 | 7.21 | 7.42 | 7.41 | 7.48 | 8.31 |
| Acid oxides [%] | 77.12 | 77.51 | 77.34 | 77.78 | 77.15 | 76.89 | 76.95 | 75.08 |

The selection of oxide composition of experimentally tested glazes took into account their position in the ternary diagram having as reference points the molar concentration of basic, acid and amphoteric oxides [12], as given in Fig. 1.

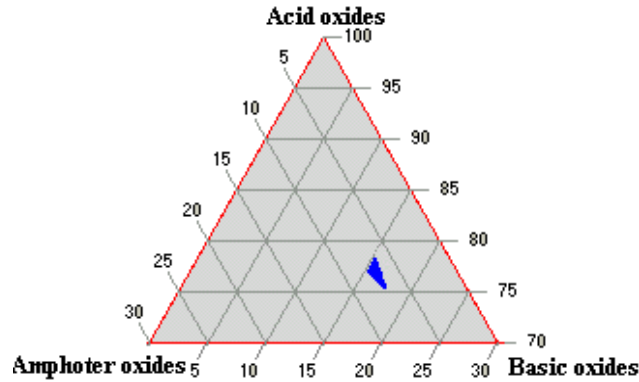


Fig. 1: Molar Gibbs diagram

The selection of glazes A – H has been done in order to establish the relationships between their composition and heat treatment behaviour through the finished aspect of glaze layer surface.

Calculation of both glaze compositions and properties was performed using mathematical models and related softwares (Glas, Matrix V5, Insight, Glasurkalkulation) [4, 13, 14]. The optimisation target was the cost (selection of economical cheapest solutions).

There were calculated the following properties: Lengersdorff firing temperature FT (equation 2) and temperatures at which the glaze reaches the characteristic points of the heat treatment, namely: glass transition temperature – T_g and softening temperature of glaze – T_s (Appendix, equation 4) – Table 2.

Table 2.

Calculated properties of glazes

| Nr. crt. | Property | Glazes | | | | | | | |
|----------|------------|--------|-------|-------|-------|-------|-------|-------|-------|
| | | (A) | (B) | (C) | (D) | (E) | (F) | (G) | (H) |
| 1 | FT [°C] | 1349 | 1357 | 1363 | 1372 | 1378 | 1373 | 1364 | 1352 |
| 2 | T_g [°C] | 638 | 628,5 | 639,6 | 637,1 | 642,1 | 626,4 | 634,2 | 655,3 |
| 3 | T_s [°C] | 745,5 | 742,6 | 742,6 | 752,7 | 750,4 | 744,2 | 747,3 | 756,6 |

The glazes A – H were prepared from unfritted raw materials: sand, feldspar (Na and K), marble, dolomite, calcined kaolin, green kaolin. The combined grinding (ball and micronisation milling) resulted a mean diameter of 9 μm , the grains size and the size distribution influencing glaze behaviour during the heat treatment.

The performed thermal analysis was focussed on the heating curve of the industrial fast firing for the glaze of tableware porcelain (5 hours cycle from cold to cold) at maximum temperature of 1390°C and a heating rate of 10°C/min. – see Fig. 2.

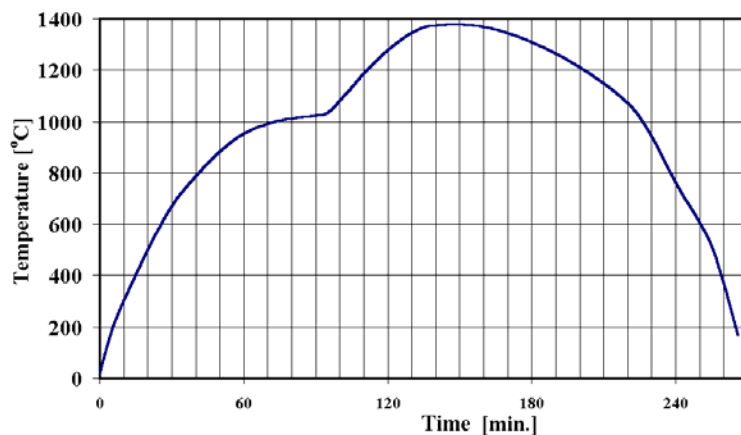


Fig. 2: Firing curve applied to glazes

Hot stage microscopy has been used for direct characterisation of melting behaviour of glazes. Cubic glaze samples ($15 \times 15 \times 15 \text{ mm}^3$) were pressed to be analysed with Leitz – Wetzlar high temperature optical microscope. Dimensional changes up to $\pm 1\%$ were recorded for every step of 10°C (at heating) based on the firing curve described in Fig. 2.

The thermal expansion was determined with a Leitz – Wetzlar dilatometer (Al_2O_3 – as reference sample) using rods of 25 mm length, prepared from melted glaze according to the firing curve. From dilatometric curves there were determined the characteristic points concerning viscosity of glazes (Table 2): glass transition temperature (T_g) and softening temperature of glaze (T_s) (Appendix, Fig. 9).

2. Results and discussions

There were recorded images of the evolution of the samples characteristics analysed with hot stage microscopy. For instance, in Fig. 3 are presented the characteristics points for glaze E.

The images were used to measure the height of the samples and then related to their initial height (Figs. 4 and 5).

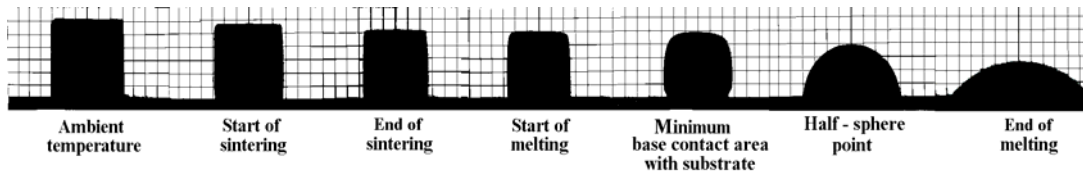


Fig. 3: Characteristic points observed by optical hot stage microscopy for glaze E sample

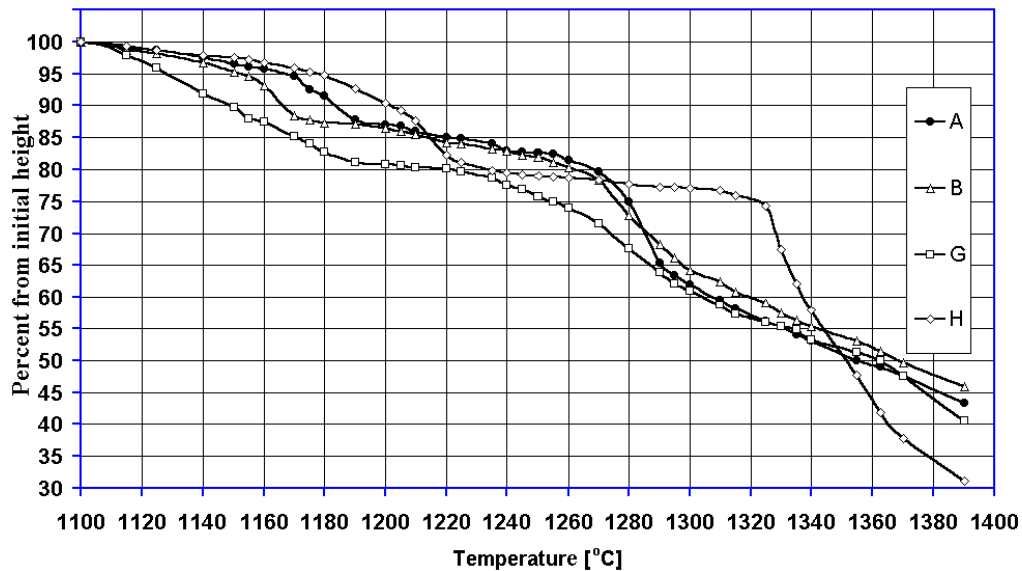


Fig. 4: Curves showing dimensional decrease against temperature of glaze samples A, B, G and H

Figs. 4 and 5 show the percentage decrease of sample's height related to its initial height, and emphasise equilibrium between gravitational, viscous and surface forces that act during the melting process upon the glaze sample. In the temperature range 1220 – 1230°C the glazes with high alumina content (E, F, H) stop the flowing probably due to Al_2O_3 dissolution.

To characterise and compare the glaze samples, their characteristic point temperatures were listed in Table 3 (see also Fig. 3).

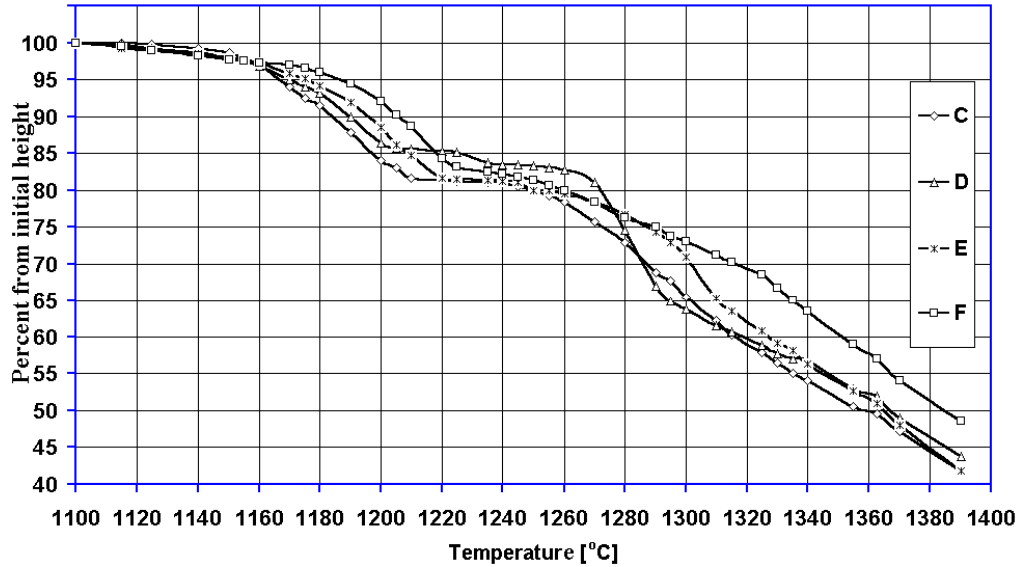


Fig. 5: Curves showing dimensional decrease against temperature of glaze samples C, D, E and F

Table 3.

Temperatures in characteristic points during glaze samples firing

| Glaze | Temperatures in characteristic points during glaze samples firing [°C] | | | | | |
|-------|--|------------------|------------------|--|---------------------------------------|----------------|
| | Start of sintering | End of sintering | Start of melting | Minimum base contact area with substrate | Half-sphere point [T _{1/2}] | End of melting |
| A | 1125 | 1165 | 1190 | 1235 | 1355 | 1380 |
| B | 1115 | 1154 | 1178 | 1255 | 1367 | 1390 |
| C | 1150 | 1161 | 1190 | 1260 | 1356 | 1380 |
| D | 1135 | 1167 | 1195 | 1235 | 1357 | 1385 |
| E | 1135 | 1175 | 1200 | 1270 | 1365 | 1380 |
| F | 1135 | 1192 | 1210 | 1270 | 1385 | 1395 |
| G | 1110 | 1125 | 1160 | 1225 | 1360 | 1380 |
| H | 1125 | 1175 | 1210 | 1300 | 1352 | 1360 |

These points determined from Figs. 4 and 5 were established, as follows: start of sintering (1% decrease from the initial height of sample), end of sintering (4-6% decrease), start of melting (12-12,5% decrease of initial height) and melting point corresponding to the minimum base contact area with the substrate (end of initial melting) stage: 16-23% decrease of initial height), half-sphere point – T_{1/2} (50% decrease of the initial height), point of melting end (54-56% decrease of the initial height of sample).

Another parameter using the tangent to the external surface of microscopy images was the contact angle between the glaze samples and the substrate (Figs 6 and 7).

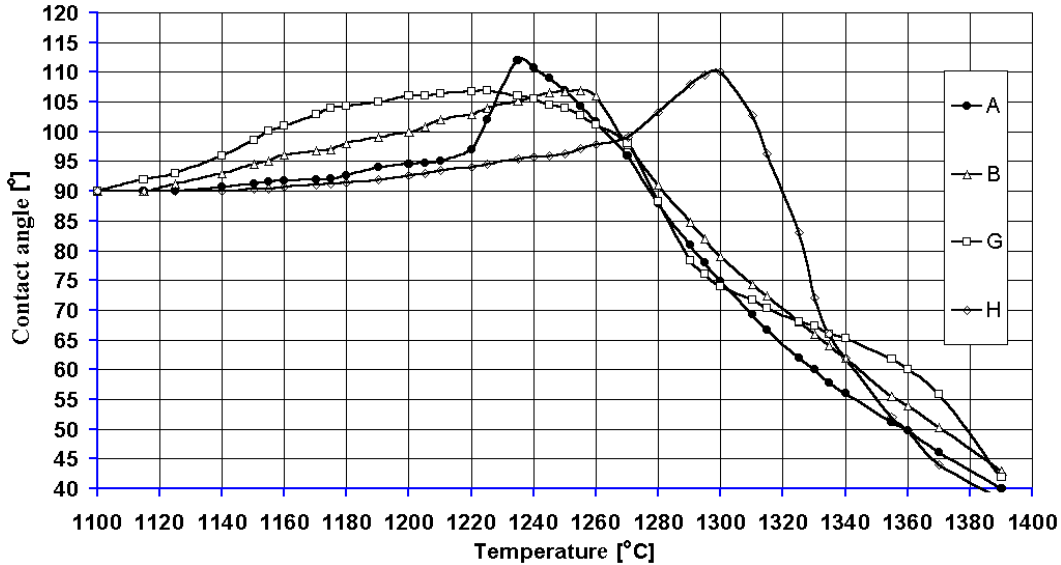


Fig. 6: Variation with temperature of contact angles for glaze samples A, B, G and H

During the melting, the glaze sample is formed of a composite phase mixture – solid and liquid. When liquid phase appears one can notice a small contraction of the sample (rounding) at the contact area between glaze and refractory substrate. The contact angle (θ) between the glaze and the substrate increases with temperature in the initial stage of melting and the shape of the sample turns towards spherical. The highest degree of spherical shape is achieved in the moment when the contact base area with the substrate reaches a minimum and the corresponding contact angle θ is maximum (Table 4) at related temperature, respectively (according to Figs. 6 and 7); at this temperature it is developed an amount of melt correlated with internal interface forces, solid – liquid, able to determine a maximum cohesion of the sample.

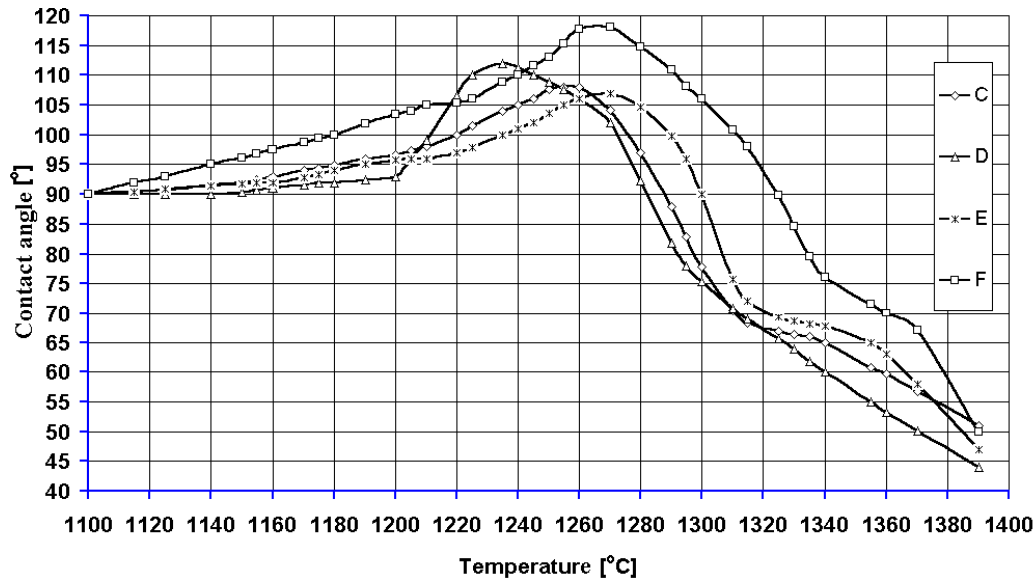


Fig. 7: Variation with temperature of contact angles for glaze samples C, D, E and F

Table 4.

Contact angle of glaze samples for the minimum base contact area with substrate

| Glaze | A | B | C | D | E | F | G | H |
|-------------------|-----|-----|-----|-----|-----|-----|-----|-----|
| Contact angle [°] | 112 | 107 | 108 | 112 | 107 | 118 | 107 | 110 |

Increasing further the temperature, while increasing the amount of melt and decreasing its viscosity, the internal interface forces will lower and, consequently, the cohesion forces. In this stage of the process, the contact glaze – substrate interface forces will increase. The contact angle (θ) between glaze sample and substrate decreases due to wetting; the sample is passing through the half – sphere point corresponding for $\theta = 90^\circ$. When increasing the temperature above the corresponding one to half – sphere point, the contact angle is becoming smaller than 90° . At complete melting of glaze, the contact angle (θ) ranges between 43° and 54° , depending on composition.

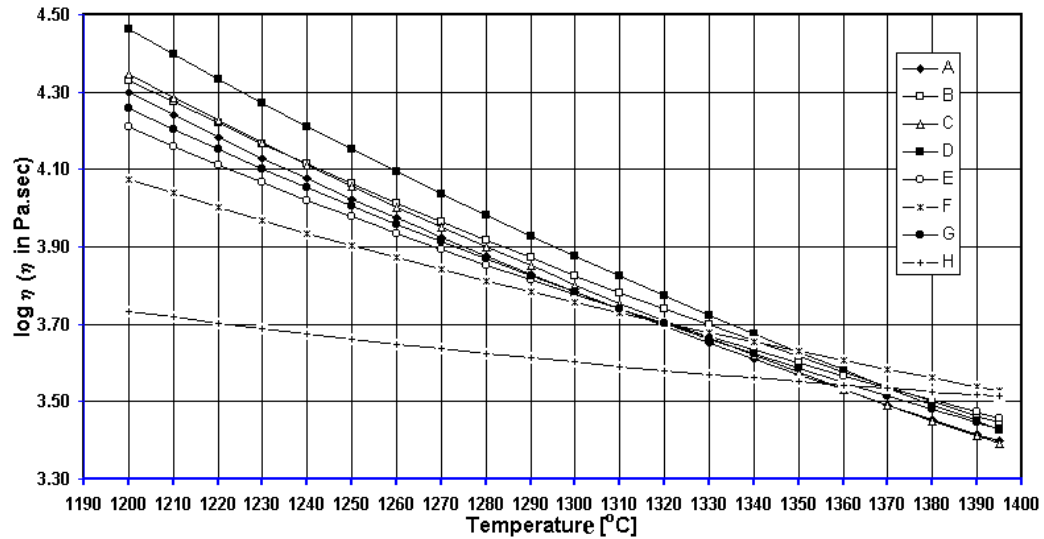
By dilatometry there were determined the temperatures T_g and T_s and hot stage microscopy provided the temperature $T_{1/2}$ of the half – sphere point (see Table 3). The corresponding values were used to calculate the constants A, B and T_0 (see Table 5) based on equations (5) – (7).

Table 5.

Measured reference temperatures and calculated constants of VFT equation

| | Glazes | | | | | | | |
|----------------|---------|---------|---------|---------|---------|---------|---------|--------|
| | A | B | C | D | E | F | G | H |
| T_g [°C] | 733 | 720 | 727 | 730 | 735 | 743 | 727 | 773 |
| T_s [°C] | 810 | 800 | 810 | 820 | 800 | 790 | 800 | 790 |
| $T_{1/2}$ [°C] | 1355 | 1367 | 1356 | 1367 | 1365 | 1385 | 1360 | 1352 |
| T_o [°C] | 475.42 | 452.58 | 437.64 | 400.33 | 537.73 | 617.31 | 492.65 | 734.27 |
| A | 0.0507 | 0.0574 | -0.3373 | -0.8231 | 0.9041 | 1.8956 | 0.4216 | 2.9848 |
| B | 3077.89 | 3193.70 | 3569.94 | 4227.34 | 2188.84 | 1270.05 | 2713.46 | 349.17 |

Log η was calculated using equation (3) and its variation with temperature (range 1200 – 1395°C) is plotted in Fig. 8.

Fig. 8: Log η variation with temperature for glaze samples A-H, between 1200 – 1395°C

Conclusions

According to our study some significant conclusions can be drawn as concern the choosing the composition of glazes based on their fusibility, in fast firing conditions applied at industrial manufacturing of hard feldspar porcelain:

- based on optical hot stage microscopy it is performed a selection of compositions whose initial melting temperatures are above 1250°C and the ending point of melting temperature ranges between 1360 – 1390°C; from glaze compositions A – H there were selected the glazes B, C, E and H;

- combining the results provided by dilatometry and optical high temperature microscopy one can select the compositions whose viscosity decreases rapidly up to 1300°C, allowing so the obtaining of a smooth fired surface of glaze. From fig. 8 is to be seen that this constrain leads to selection of only glazes B, C and E, as the low viscosity of glaze H at 1250°C makes glaze to flow from the product edges during manufacture (firing) process;
- the firing curves applied to glazes can be designed as function of fusibility of precursor mixtures and, consequently, using information provided by high temperature microscopy and dilatometry, as well;
- for the characteristic temperatures of the heat treatment (firing process) applied to glazes (T_g and T_s) there were noticed differences between the calculated values (according to equation 4 from Appendix – Table 2) and the measured values (Table 5). For T_g , experimental values are with 85 – 120°C higher then the calculated ones and for T_s with 30 – 70°C.

Appendix

To calculate the temperatures for which $\log \eta$ has the values from the reference points, it was used the method of Rodriguez Cuartas with aid of Glas program [4], according to relation:

$$T_i = \sum_{j=1}^n \frac{c_j \cdot P_j}{P_{SiO_2}}, \quad (4)$$

where p_j is the weight percentage of “j”-th oxide and c_j are coefficients specific to each oxide and each temperature [4].

Viscosity of melt can be estimated from dilatometric and high temperature microscopy measurements using three known reference points [15-20]:

- **Glass transition temperature (T_g)**, emphasising the point of difference between plastic state and hardened glass state, that is accepted for all silicate glasses [15-17] as the temperature at which $\eta = 10^{12}$ Pa.sec.
- **Dilatometric softening temperature of glaze (T_s)**, highlighting the point at which the speed of glaze deformation due to viscous flow equals dilatation, the corresponding values ranging as function of composition between $10^8 - 10^{10}$ Pa.sec [18-19]. Margini et coll. [17] have determined the viscosity at T_s for glazes and frits used for preparation of multi – oxide / silicate glazes as $\eta = 10^{9.25}$ Pa.sec. Fig. 9 shows the reference points of thermal expansion curve (T_g and T_s) used for viscosity calculation of glazes.

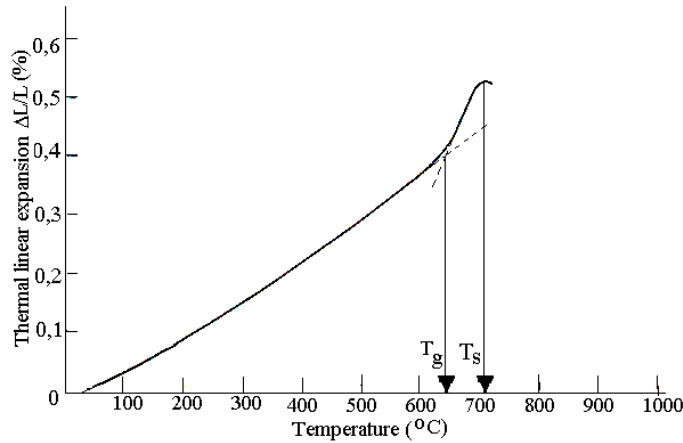


Fig. 9: T_g and T_s determination through dilatometric method:
 L = initial sample length, ΔL = sample length change

- **Temperature of half – sphere point ($T_{1/2}$)** represents the temperature at which the sample forms a half – sphere during the hot stage microscopy analysis (Fig. 3). This half – sphere point is achieved when the height of the sample represents half from the base length and the contact angle $\theta = 90^\circ$. The value of viscosity at $T_{1/2}$ ($\eta=10^{3.55}$ Pa.sec) has been considered according to [20]. This reference point has been chosen due to the simple recognition of shape provided by accurate measurements.

For industrial usage, the above mentioned three quantified reference points - evaluated based on specified criteria can be used for glaze viscosity calculation through VFT equation, the three constants, namely A, B, and T_0 , as follows [21]:

$$T_0 = \frac{12T_g - 3.55T_{1/2} + (9.25T_s - 12T_g) \frac{T_{1/2} - T_g}{T_s - T_g}}{8.45 - 2.75 \frac{T_{1/2} - T_g}{T_s - T_g}}, \quad (5)$$

$$A = (9.25T_s - 12T_g + 2.75T_0) / (T_s - T_g), \quad (6)$$

$$B = (T_g - T_0)(12 - A), \quad (7)$$

where the temperatures are expressed in Celsius degrees and coefficients and constants are related to viscosity, being expressed in Pa.sec.

Glaze viscosity, at the maximum firing temperature that allows a proper distribution of melt on the surface to be glazed, should range in the optimum domain of $10^3 - 10^4$ Pa.sec [22].

REFERENCES

1. *M. Wimer* – *Keramische Zeitschrift* 8, **43**, 1991, 663-666
2. *C.E. Villa, D.R. Dinger, J.E. Funk* – *Interceram* 5-6, **46**, 1997, 303-308
3. *M. Preda* – *Ceramic and Refractory*, Printech Publishing House, Bucharest, 2001 (in Romanian)
4. *H.H. Rehner, M. Preda* – *Building Materials* 3, **27**, 1997, 164-170
5. *I. Teoreanu, N. Ciocea, A. Barbulescu, N. Ciontea* - *Ceramic and Refractory products Technology*, Ed. Tehnică Publishing House, Bucharest, 1985 (in Romanian)
6. *W. Eithel* – *Silicate science, glasses, enamels, slags*, vol II, Academic press, New York, 1965
7. *P. Balta* – *Glass Technology*, 2nd- edition, Ed. Didactica & Pedagogica Publishing House, Bucharest, 1984 (in Romanian)
8. *D. Fortuna, A. Angeli* - *cfi/Ber. DKG* 1-2, **81**, 2004, 26-30
9. *H. Mortel, St. Krebs, K. Pham-Gia* – *cfi/Ber DKG* 5, **77**, 2000, 26-31
10. *H. Mortel, H. J. Oel, G. Preidt* – *Interceram* 1, **36**, 1987, 26-28
11. *W. Schulle* – *Interceram* 4, **52**, 2003, 192-196
12. *Web reference* - <http://www.dhpot.demon.co.uk/eutectics.htm>
13. *Web reference* - <http://digitalfire.com/> INSIGHT 5.4, Ceramic Chemistry Software
14. *Web reference* - <http://www.Matrix2000.co.nz>, MATRIX V 5, Glaze software
15. *M. Paganelli* - *Ind. Ceram.* 2, **17**, 1997, 69-73
16. *A. R. Boccaccini, B. Hamann* - *J. Mater. Sci.* 3, **36**, 1999, 5419-5436
17. *F. Margini, R. Ferrari, P. Brunetti* – *Ceramica Informazione* 171, 1980, 391-398
18. *J. E. Shelby* - *Introduction to Glass Science and Technology*, Royal Society of Chemistry, Cambridge, U.K., 1997.
19. *Web reference* - <http://www.sciglass.com/glossary/html/glos5qhx.htm>, SciGlass Glossary.
20. *M.J.Pascual, L.Pascual, A.Duran* - *Phys. Chem. Glasses* 1, **42**, 2001, 61-66
21. *M. Ahmed, D. A. Earl* - *Am. Ceram. Soc. Bull.* 3, **81**, 2002, 47-51
22. *B. Burzacchini, M. Paganelli, G.C. Heinrich* - *Ceram. Eng. Sci. Proc.* 1, **17**, 1996, 60-66